Electronic Supplementary Material (ESI) for Nanoscale.
This journal is © The Royal Society of Chemistry 2016

Supporting Information

Constructing bifunctional nanoparticles for dual targeting: Improved grafting and surface recognition assessment of multiple ligand nanoparticles

Maria Cristina Lo Giudice, Fabian Meder, Ester Polo, Steffi S. Thomas, Kholoud Alnahdi, Sandra Lara, Kenneth A. Dawson**

Table of Contents

3. Literature

1. Materials and Methods

1.1 Materials

General chemicals

Tetraethylorthosilicate (TEOS, 99%, product no. 86578), (3-mercaptopropyl) trimethoxysilane (MPTMS, 95 %, product no. 175617), Dimethyl sulfoxide (DMSO,>99.9%, product no. 276855), Skimmed milk powder (product no. 70166), Sodium dodecyl sulfate (product no. L3771), Glycine (product no. G8898), Ammonium persulfate (product no. A3678), Trizma base (product no. T1503), Tween 20 (product no. P1379), N,N,N′,N′-Tetramethylethylenediamine (product no. T9281), Acrylamide/bis-acrylamide,40% solution (product no. A7802), DL-Dithiothreitol (product no. D5545), Ethanol (product no. 32294-2), Methanol (product no. 24229-2). 3-Mercaptopropionic acid (product no. M5801), Cadmium chloride (product no. 02908), Hydrogen tetrachloroaurate(III) (product no. 520918), 4-Aminophenyl β-D-galactopyranoside (product no. A9545), Sodium borohydride (product no. S9125), N-(3-Dimethylaminopropyl)-N′--ethylcarbodiimide hydrochloride (product no. E6383), N-Hydroxysulfosuccinimide sodium salt (product no. 56485), Methoxypolyethylene glycol amine (product no. 07964) were purchased from Sigma Aldrich, Ireland. Dibenzylcyclooctyne-Cy5.5 (DBCO-Cy5.5 product no. CLK-1046) from Jena Bioscience, Germany, 3-azidopropyltriethoxysilane (N3PTES, product no. AB268770) from ABCR GmbH, Germany, and Ammonium hydroxide (35%,product no. 10000030) from Thermo Fisher, Ireland. Color Plus Pre-stained Protein Ladder, Broad Range (10-230 kDa) (product no. P7711S) and Blue Loading Buffer for SDS-PAGE were purchased from New England Bio-Labs (product no. B77035). PVC calibration standard for DCS measurements 483 nm (product no. PS000483) was ordered from Analytik Ltd. BCA

Protein Assay Kit (product no. 23227) Tellurium, 99.8%, powder (product no. 315990250) was purchased from Acros Organics.

PEG-linker

Maleimide-$PEG_{(8)}$-NHS (Thermo Scientific, Ireland, product no. 22108) was purchased from Thermo Scientific, Ireland. DBCO-$PEG_{(40)}$-NHS (MW 2000 Dalton, product no. PG2-DBNS-2k) , Maleimide-$PEG_{(40)}$-NHS (MW 2000 Dalton, product no. PG2-MLNS-2k) was purchased from Nanocs, UK. Dibenzylcyclooctyne-PEG_4-Alcohol (DBCO-PEG_4-OH, product no. CLK-A104-25) was purchased from Jena Bioscience, Germany, alpha-Methoxy-omega-maleinimido tetra(ethylene glycol) (maleimide-PEG_4, product no. PEG2375) and alpha-Methoxy-omega-ethyl-maleinimide poly(ethylene glycol) (MW 5000 Dalton) (maleimide-$PEG_{(80)}$, product no. PEG1149.0001) were purchased from Iris Biotech GmbH, Germany.

Proteins

Human holo-Transferrin (Tf, >98%, product no. T4132), Human serum albumin (HSA, >99%, product no. A8763), Bovine serum albumin (product no. A8763A2153) were purchased from Sigma Aldrich, Ireland . Recombinant Epidermal growth factor made in *E. coli* (EGF, >95%, product no. YSP1136) was ordered from Speed Biosystems, USA. Transferrin From Human Serum, Alexa Fluor® 488 Conjugate (product no. T13342) and Epidermal Growth Factor, Biotinylated, complexed to Alexa Fluor® 488 Streptavidin (Alexa Fluor® 488 EGF complex) (product no. E13345) and Goat anti-Mouse IgG (H+L) Secondary Antibody, Alexa Fluor® 488 conjugate (product no. A11029) were ordered from Thermo-Scientific. Anti-Transferrin antibody [HTF-14] (product no. ab769) Anti-Human Serum Albumin antibody (product no. ab113636) and anti-R Phycoerythrin antibody (product no. ab117263) were purchased from AbCam. EGF Antibody (F-9) (product no. sc-166779) was obtained from Santa Cruz Biotechnology. *Buffers and water*

HEPES buffer, 20 mM, adjusted to pH 7.2, 0.2 µm sterile filtered, (Sigma Aldrich, Ireland, product no. H4034).

Phosphate buffered saline, PBS buffer, 10 mM, pH 7.4, 0.2 µm sterile filtered (Sigma Aldrich, Ireland ,product no. P4417).

Water used in all experiments was ultrapure water obtained by a Milli-Q purification system (Millipore Corporation, Ireland).

1.2 Synthesis of SiNPs

Fluorescent core-shell SiNP (~65 nm, number average) where synthesized as described in an earlier publication [1]. Non-fluorescent SiNPs of similar size (~68 nm, number average) were prepared using the method described by Huang *et al.* and by adding 1.52 mL TEOS in a mixture of 33.4 mL methanol, 3.75 mL ammonium hydroxide, and 3.1 mL water and reaction for 3 hours at 40°C under magnetic stirring. [2] After synthesis, SiNPs were washed once with ethanol and 3 times with water by repeated centrifugation (15 min, 20000 rcf) and ultrasonic bath-assisted resuspension for purification and filtered through a 0.45 µm sterile filter. Particle concentrations were determined by measuring the dry weight in triplicates.

1.3 Surface functionalization with thiol and azide groups

For surface functionalization with thiol and azide groups, 9 ml of a 8.7 mg*mL^{-1} of SiNPs in water were stirred and mixed with 0.5 mL of ethanol containing either 16.3 µL of MPTMS or 21.6 µL N3PTES for monofunctional surface chemistry or both solutions for bifunctional surface chemistry and stirred for 60 min at 25 °C and subsequently reacted at 90 °C for 60 min under continuous stirring at 600 rpm. The amounts of silanes added correspond to ~3 times a monolayer of silane molecules related to the SiNP surface area.

The particles were cooled to room temperature and subsequently washed 3 times with water by repeated centrifugation (20000 rcf, 15 min) and ultrasonic bath assisted redispersion for purification. Subsequently the functionalized SiNPs were centrifuged again at 3000 rcf for 3 minutes to sediment any larger species and the supernatant was taken as the final SiNP dispersion. The concentration was determined by measuring the dry weight in triplicates and functionalized SiNPs were used within 24 hours of preparation and stored during this period at 4°C in the dark.

1.4 Protein conjugation

Surface functionalized SiNPs were transferred in HEPES buffer by 15 min centrifugation (20000 rcf) and resuspended in the buffer in an ultrasonic bath.

Protein PEGylation. An amount of Tf, HSA, and EGF which corresponds to a theoretical monolayer of the protein related to the surface area of the SiNPs to be added was weighed and dissolved in HEPES buffer (the protein monolayer was calculated assuming regular cubic packing of spheres with a diameter corresponding to the longest protein dimension obtained from the protein crystal structure of the protein data base (PDB) entries number 1H76 for Tf, 1EGF for EGF, and 1E7I for HSA[3], respectively on the total particle surface area which was calculated assuming an average particle diameter of 65 nm and taking into account the added weight of particles and the density of silica of 2 $g*cm^{-3}$). Then, the bifunctional PEG linker, either NHS-$PEG_{(40)}$-R or NHS-$PEG_{(8)}$-maleimide (R= maleimide or DBCO for thiol- or azide-functionalized SiNPs, respectively) were added from a stock solution of the PEG in dimethyl sulfoxide (DMSO) that has been dissolved in 1 mL HEPES buffer just before addition to the proteins in a ratio of 10 PEG linker per HSA or Tf molecule and 2 PEG linker per EGF molecule to separate solutions of the proteins and stirred for 120 min at 22°C to obtain PEGylated Tf, EGF, or HSA (due to the

smaller size of EGF less PEG per protein was added to avoid excessive PEGylation which may influence recognition).

SiNP-protein conjugation. For linking strategy A, either PEGylated, maleimide functional Tf, HSA, or EGF were added to the thiol-functionalized SiNPs in HEPES to obtain monofunctional particles. To obtain bifunctional particles, two solutions of the PEGylated protein (Tf and HSA or Tf and EGF, respectively) were mixed in the volumes to add one theoretical monolayer of each protein and then added to the thiol-functional SiNPs. For Strategy B, PEGylated, DBCO-functional Tf was added to azide-functionalized SiNPs, PEGylated, maleimide functional EGF to thiol-functionalized SiNPs to obtain monofunctional SiNPs and to obtain bifunctional SiNPs-DBCO functional Tf and maleimide functional EGF were mixed and added to SiNPs functionalized with both, azide and thiol groups. The ratio between SiNPs and proteins always corresponded to a theoretical monolayer of protein on the surface of the SiNPs as described above. Table S1 summarizes the amounts used. Then the particles were magnetically stirred (500 rpm) at 22°C for 120 min. When no "backfilling" was conducted, the SiNP-protein conjugates were subsequently washed three times with PBS by repeated centrifugation at 15000 rcf for 10 min and resuspension in PBS with aid of repeated pipetting in an ultrasound bath for 20 sec.

Backfilling. When backfilling was conducted, R-$PEG_{(4)}$-OH or R-$PEG_{(80)}$ (R = maleimide for thiol-functional core SiNPs and DBCO for azide-functional core SiNPs, for bifunctional, azide- and thiol- functional core SiNPs, a one to one mixture of maleimide- and azide-PEG was used) were dissolved in 50 µL HEPES buffer from a stock solution in DMSO in the concentrations given in Table S1 (in excess to thiol or azide groups, respectively) and added to the SiNP-protein conjugates and magnetically stirred (500 rpm) at 22°C for 120 min. Afterwards, the conjugates were washed into PBS as described above. Concentrations of SiNP-protein conjugates having a fluorescent SiNP core were

determined by measuring the specific fluorescence profile and comparing known particle concentration standards of unfunctionalized fluorescent core particles. Concentrations of SiNP-protein conjugates with an unlabeled, non-fluorescent core SiNP have been obtained by three times determination of the dry weight of 200 µL of the particles in an ultra-balance (Cubis® Ultramicro, Satorius, Ireland) and subtracting the dry weight of 200 µL PBS.

Table S1 overview of ratio and composition of SiNP-protein conjugation reactions.

	Monofunctional SiNP Tf, strategy A	**Monofunctional SiNP HSA, strategy A**	**Bifunctional SiNP Tf HSA ratio 1:1, strategy A**	**Bifunctional SiNP Tf HSA ratio 3:1, strategy A**	**Monofunctional SiNP Tf, strategy B**	**Monofunctional SiNP EGF, strategy B**	**Bifunctional SiNP Tf EGF 1:1, strategy B**	**Monofunctional SiNP Tf, strategy A**	**Monofunctional SiNP EGF, strategy A**	**Bifunctional SiNP Tf EGF 1:1, strategy A**
SiNPs	4 mL of 8.5 mg*mL^{-1} thiol-SiNP	4 mL of 8.5 mg*mL^{-1} thiol-SiNP	4 mL of 8.5 mg*mL^{-1} thiol-SiNP	4 mL of 8.5 mg*mL^{-1} thiol-SiNP	6 mL of 6 mg*mL^{-1} azide-SiNP	6 mL of 6 mg*mL^{-1} thiol-SiNP	6 mL of 6 mg*mL^{-1} thiol&azide-SiNP	6 mL of 6 mg*mL^{-1} thiol-SiNP	6 mL of 6 mg*mL^{-1} thiol-SiNP	6 mL of 6 mg*mL^{-1} thiol-SiNP
PEG-ylated Tf	4 mL of 1.2 mg*mL^{-1} (maleimide PEG_8-Tf)	-	4 mL of 1.2 mg*mL^{-1} (maleimide PEG_8-Tf)	12 mL of 1.2 mg*mL^{-1} (maleimide PEG_8-Tf)	6 mL of 1.2 mg*mL^{-1} (DBCO PEG_{40}-Tf)	-	6 mL of 1.2 mg*mL^{-1} (DBCO PEG_{40}-Tf)	6 mL of 1.2 mg*mL^{-1} (maleimide PEG_{40}-Tf)	-	6 mL of 1.2 mg*mL^{-1} (maleimide PEG_{40}-Tf)
PEG-ylated HSA	-	4 mL of 1.0 mg*mL^{-1} (maleimide PEG_8-HSA)	4 mL of 1.0 mg*mL^{-1} (maleimide PEG_8-HSA)	4 mL of 1.0 mg*mL^{-1} (maleimide PEG_8-HSA)	-	-	-	-	-	-
PEG-ylated EGF	-	-	-	-	-	6 mL of 0.24 mg*mL^{-1} (maleimide PEG_{40}-EGF)	6 mL of 0.24 mg*mL^{-1} (maleimide PEG_{40}-EGF)	-	6 mL of 0.24 mg*mL^{-1} (maleimide PEG_{40}-EGF)	6 mL of 0.24 mg*mL^{-1} (maleimide PEG_{40}-EGF)
Back-filling PEG	-	-	-	-	1.1 mg in 50 µL HEPES (DBCO PEG_4-OH)	0.72 mg in 50 µL HEPES (maleimide PEG_4)	1.1 mg DBCO PEG_4-OH in and 0.72 mg maleimide PEG_4 in 100 µL HEPES	9.0 mg in 50 µL HEPES (maleimide PEG_{80})	9.0 mg in 50 µL HEPES (maleimide PEG_{80})	9.0 mg in 50 µL HEPES (maleimide PEG_{80})

1.5 Determination of depleted proteins during conjugation reaction by gel electrophoresis

To determine the amount of protein conjugated to the particles, we compared the supernatant of the reaction solution containing the unbound protein (after removing SiNP-protein conjugates via centrifugation for 15 min at 20000 rcf) with a solution containing same initial amounts of PEGylated proteins but no particles using sodium dodecyl sulfate polyacrylamide gel electrophoresis (SDS-PAGE) and assume that the difference, the depleted protein, is conjugated to the particles. Fifty µL of the supernatants (and references) were diluted by adding 50 µL PBS. In addition, standards were prepared by mixing PEGylated Tf and HSA or Tf and EGF (depending on which proteins were conjugated to the SiNPs) in known concentrations. Then, 10 µL of the sample or the standard were mixed with 4.5 µL of 3X SDS Blue Loading Buffer (New England BioLabs, UK, product No. B7703S) premixed with 0.5 µL 30X Reducing Agent 1.25 M DTT (New England BioLabs, UK, product No. B7703S) and vortexed. The samples were heated for 10 minutes at 100°C and subsequently loaded into 15-well 4-15 % Mini-PROTEAN® TGX™ Precast Gels (Biorad, Ireland, product No. 4561086) or self-casted 15-well gels with a 4 % acrylamide stacking gel and a 10 % acrylamide separation gel. The gels were run for 45 min in a Mini-PROTEAN Tetra Cell (Biorad, Ireland) at 130 V using a 10 mM Tris, 10 mM Tricine, 0.01% SDS running buffer. Gels were stained using Comassie blue staining as described in ref. [4]. The band intensity was quantified using ImageJ3 (Version 1.47v) after the gels were imaged in a Syngene G-Box gel documentation system (Syngene, UK) and transilluminating the gels with UV light. Average and standard deviation of analysis of three gels per sample are reported.

The quantification of adsorbed and desorbed proteins was done as follows. To quantify the bound protein amounts, the intensity of the corresponding bands in the sample was compared with the corresponding reference with known protein concentrations. The relative decrease of the band intensity was then used to calculate the depleted protein.

Single bands were obtained for each protein and linear standard curves within 5-200 $\mu g*mL^{-1}$ for Tf, 7-40 $\mu g*mL^{-1}$ EGF, and 8-170 $\mu g*mL^{-1}$ HSA for Coomassie staining.

1.6 Determination of conjugated proteins by HPLC

To confirm that the protein concentrations obtained by analyzing the depleted proteins in SDS-PAGE resemble the surface-bound proteins, we performed an HPLC analysis of the amino acids after acid digestion of the SiNP-protein conjugates (24 hours 6M HCL, 100 °C under vacuum) as described by ref. [5]. Four ml of SiNP-protein conjugates (3 $mg*ml^{-1}$) were concentrated into 1 mL PBS, then 10 µL of a 10 $\mu mol*mL^{-1}$ norvaline solution in PBS (norvaline was added to each sample in fixed concentration as an internal reference to which measured amino acid profiles were normalized) and 1 mL of 12 M HCl were added. The solution was transferred into a vacuum glass tube, exposed to vacuum and then flushed with nitrogen (repeated three times), then evacuated, sealed and heated at 110 °C for 24 hours. Subsequently, the solutions were centrifuged to sediment any SiNP residues and obtain a supernatant containing the amino acids of the conjugated proteins. The supernatant, 1.65 mL, was dried under vacuum and the dry product was dissolved in 0.1 mL water. The amino acid profiles were analyzed after derivatization with o-Phthaldildehyde (OPA, Sigma Aldrich, Ireland, product no. P0657) reagent (prepared according to ref. [5]) in an Agilent 1100 HPLC (Agilent, Ireland) with a ZORBAX Eclipse XDB C18 (4.6x150 mm, 5µm) column using a binary gradient mobile phase consisting of mobile phase A (2.8 g anhydrous Na_2HPO_4, 7.6 g $Na_2B_4O_7*10\ H_2O$, and 16 mg NaN_3 in 2 L H_2O adjusted to pH 8.15) and mobile phase B (methanol:acetonitrile:water, 9:9:2, v:v:v) as detailed in ref. [6]. For labelling, 30 µL of the OPA solution was mixed with 10 µl of the sample in an automated program of an automatic sampler and then injected. Detection of OPA-labeled amino acids was done by measuring absorbance at 338 nm using an

Agilent 1260 Infinity Diode Array Detector (Agilent, Ireland). To identify the amino acids, retention times of single amino acids standards were determined under same conditions as the samples. Known concentrations of Tf and EGF were digested and measured in the same way as the SiNP-conjugates to obtain their amino acid profile. The peak areas in the chromatograms of 15 amino acids (ASP, GLU, SER, HIS, GLY, THR, ARG, ALA, VAL, MET, NOR, PHE, ILE, LEU, LYS) were analyzed using the instrument software (ChemStation, Version B.04.01). A numerical analysis of the obtained amino acid profiles was performed according to Salchert *et al.[5]* and a MATLAB code (MATLAB, Version 8.1.0.604) was used to solve a linear equation system Ax = B in which B is the amino acid profile of the sample and A is the profile of either single Tf or EGF of known concentration. As detailed in ref. [5] some amino acids were excluded from the analysis to minimize the fitting error. The solution x is the multiple of A in B and was used to obtain the ratios of Tf and EGF on bifunctional particles.

1.7 Determination of nonspecifically bound proteins

Nonspecific adsorption of Tf, HSA, and EGF on SiNPs may occur during the conjugation reaction resulting in noncovalently bound proteins. These may desorb or be replaced in a biological environment which is expected to influence the overall functionality of the SiNPs-protein conjugates.[7] To determine the amounts on nonspecifically bound proteins, SiNPs conjugate (3 $mg*m^{-1}$) and known standards of PEGylated Tf and HSA or Tf and EGF mixtures were analyzed in SDS-PAGE as described above (section 1.5). It is expected, that the denaturizing conditions during sample preparation and the electric field during electrophoresis will “pull-off” only nonspecifically bound proteins, which then enter the gel. We assume that covalently bound proteins remain on the SiNPs surface which hinders them to enter the acrylamide separation gel as the pores are smaller than the particles [8]

and as tested with florescent labelled SiNPs which were shown not to enter the gel [1]. The gels were silver stained (2D Silver Stain II Reagent, Cosmo Bio Co. Ltd., Japan, product no DCB-423413) and the amount of proteins was quantified by densitometry (as described in section 1.5) of standard curves obtained of known protein concentrations and samples analyzed in the same gel. A gel of Tf and HSA particles is shown below.

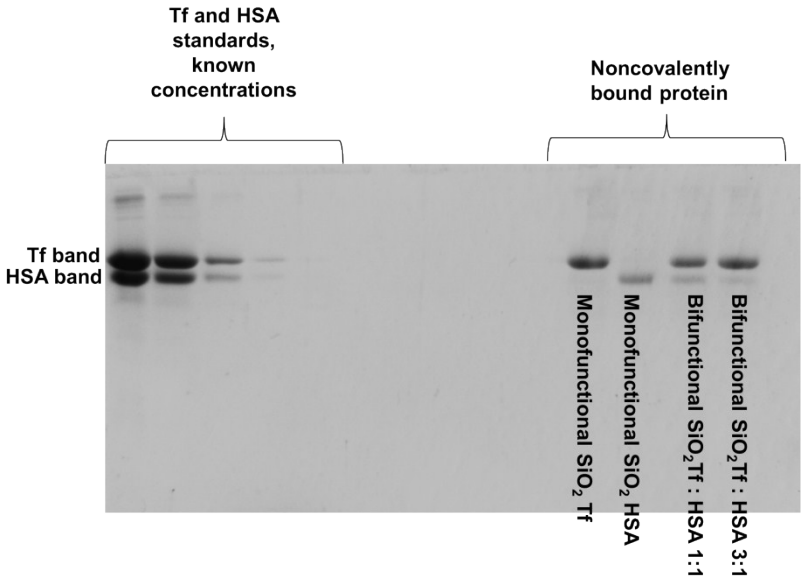

1.8 Quantification of thiol groups

Thiol-groups on SiNPs have been determined using Ellman's assay using the following protocol. A reagent buffer was prepared of 0.1 M sodium phosphate and 1 mM ethylenediaminetetraacetic acid (Sigma Aldrich, Ireland, product no. 03620) in water and adjusted to pH 8.0. Then, 4 mg 5,5'-Dithio-bis-(2-nitrobenzoic acid) (Sigma Adrich, Ireland, product no. D8130) was dissolved in 1 mL buffer to obtain a reagent solution. For the analysis, 5 µL of the reagent solution was mixed with 205 µL of buffer and 25 µL of the SiNPs (with known concentration usually between 1 and 3 $mg*mL^{-1}$) and with the samples for the standard curve using dilutions of MPTMS in ethanol in concentrations between 5 and 1500 µM and incubated for 15 min. Subsequently, the samples were

centrifuged for 20 min at 20000 rcf and the absorbance of the supernatants was measured in a plate reader (Varioskan Flash, Thermo Scientifc, Ireland). As references, bare SiNPs, azide SiNPs and the supernatant of the particles SiNPs were measured. None of the references resulted in a measurable signal. All samples were determined in triplicates and results are average and standard deviation.

1.9 Quantification of azide groups

To quantify the azide groups, 10 µL of the functionalized SiNPs (concentrated to 7 $mg*mL^{-1}$) were mixed with 90 µL H_2O and 60 µL of a 1.125 $mg*mL^{-1}$ DBCO-Cy5.5 fluorophore solution in DMSO and mixed overnight at 22 °C. The added amount of DBCO-Cy5.5 corresponds to 10 x molecular excess assuming 1 azide group per nm^2 on SiNPs. After the reaction, particles were washed four times to remove any unbound fluorophore by repeated centrifugation (15 min, 20000 rcf) and redispersion in water using an ultrasonic bath. Then the fluorescence emission at 694 nm after excitation at 678 nm was determined in a plate reader (Varioskan Flash, Thermo Scientifc). All samples were determined in triplicates and results are average and standard deviation.

1.10 Dot blot assays of SiNP-protein conjugates

A modified immuno dot blot assay was conducted as a qualitative measure of the biological recognition of the SiNP-protein conjugates. Polyvinylidene fluoride (PVDF) membrane were cut and activated by wetting in methanol for 1 minute. The membranes were then washed twice with water and twice more with PBS leaving them to equilibrate in PBS for 5 mins prior to use. Working stocks of each antibody (either monoclonal anti-Tf, monoclonal anti-EGF, or monoclonal anti-HSA) were created by diluting the antibodies to 1 mg*mL in PBS. One µL of each antibody stock was spotted onto each membrane. The

membranes were subsequently blocked with 5% casein in PBS for 1 hour at room temperature.

After blocking, the membranes were washed with PBS twice and the incubated with the SiNPs-protein conjugates (fluorescent SiNP core) at concentrations of 1 mg*mL^{-1}. The blots were incubated in the dark for one hour before washing with PBS four times and imaging on a Syngene G-Box gel documentation system (Syngene, UK).

1.11 Dot blot assays to determine cross-reactivity of antibodies

As verification of the antibodies and to determine any cross reactivity, dot blot assays were performed as follows. 4x4 cm squares of PVDF membrane were cut and activated by wetting in methanol for 1 minute. The membranes were then washed twice with Milli-Q water and twice more with PBS leaving them to equilibrate in PBS for 5 mins prior to use. 2 µL of stock solutions (1 mg*mL^{-1} in PBS) of HSA or Tf were spotted onto each membrane. The membranes were subsequently blocked by incubation with a 5% casein solution in PBS for 1 h at room temperature, under constant shaking. After blocking of the surface, the membranes were washed 3 times with PBS (pH = 7.4) and incubated for 1 h with monoclonal antibody against transferrin and human serum albumin diluted in PBS to a final concentration of 1 µg*mL^{-1}. After 3 additional washing steps in PBS, the membranes were incubated with the Alexa 488-labelled secondary antibody for 1 h in the dark, washed 5 times, to remove the unbound antibody, and let dry. To assess the cross-reactivity of the primary antibody against Tf and EGF with EGF and Tf respectively, working stocks of each antibody were created by diluting the antibodies to 200 µg*mL in PBS. 2 µL of each antibody stock was spotted onto each membrane. The membranes were subsequently blocked with 5% casein solution in PBS for 1 hour at room temperature. After blocking, the membranes were washed with PBS twice and the incubated with

fluorescent Tf or fluorescent EGF at concentrations of 5 µg*ml and 0.5 µg*mL respectively. All the membranes were imaged on a Syngene G-Box gel documentation system (Syngene, UK).

1.12 Synthesis of gold NPs (AuNPs)

A 0.0125 % w/w solution of $HAuCl_4$ was prepared (40 mL), separately from a reducing solution (10 mL) of 0.25 % w/w sodium citrate, 0.25 % w/w tannic acid and 0.05 % w/w K_2CO_3. The two solutions were pre-heated at 60˚C, then transferred to a round-bottom flask and stirring for 2-3 min at 100˚C. A color change to brown-red was noticed when the reaction was completed. To stop the reaction, the flask was initially cooled on ice, followed by cooling at room temperature. In order to functionalized the gold nanoparticles with antibodies, the citrate of the nanoparticle surface was exchanged by a O-(2-Carboxyethyl)-O′-(2-mercaptoethyl) heptaethylene glycol (SH-PEG-COOH, MW= 458.56 g/mol). Briefly, 50 mL of gold nanoparticles after synthesis were incubated overnight, under continuous stirring, with SDS (0.03%), NaOH (25 mM) and an equivalent amount of SH-PEG-COOH to obtain 5000 chains per nanoparticle. The carboxylated gold nanoparticles were washed 3 times and concentrated with centrifugal filter units (10,000 molecular weight cut-off, MWCO). The gold nanoparticles are characterized by DCS and TEM, UV-Vis spectroscopy and gel-electrophoresis.

1.13 Synthesis of quantum dots (QDs)

The synthesis of mercaptopropionic acid (MPA) protected CdTe QDs was performed following the procedure reported by S. Penades et al.[9]. A solution of 0.2 mmol of $CdCl_2$ in 40 mL of deoxygenated water was mixed with 0.34 mmol of MPA. The pH was adjusted

to pH 7 with NaOH (1N) and the solution was bubbled with Ar for 30 min. After that, 0.5mL of freshly prepared NaHTe (40 mM) was added to the three-necked flask and the temperature of the mixture was raised at 140º C. After either 90 min or 20 h stirring at 140º C, the two desired emission wavelengths were obtained, and the reaction was stopped by cooling down to room temperature. The sodium hydrogen tellurite (NaHTe) precursor was freshly synthesized following the procedure described by W. Zhong *et al.*[10] 0.196 mmol of Te powder was mixed with 0.513 mmol of $NaBH_4$ in 5mL of deoxygenated water under Ar atmosphere. The reaction was heated to 85ºC under a high flow of Ar and magnetic stirring for 45 min. The QDs were purified by precipitation with acetone. Finally, the QDs were separated by centrifugation and dialyzed 48 h against PBS buffer. The QDs particles were characterized by DCS, UV-visible adsorption spectroscopy and fluorescence spectroscopy. A fluorescence quantum yield (QY) of 18% and 20% for the green- and orange-emitting QDs respectively was calculated by comparison with a standard curve of Rhodamine RG6, according to the following formula:

$$QY = QY_{standard} \cdot \frac{F_{QD}}{F_{standard}} \cdot \frac{Abs_{standard}}{Abs_{QD}} \cdot \left(\frac{\eta_{QD}}{\eta_{standard}}\right)^2$$

where F is the area of the photoluminescence peak of QDs and standard (excitaion wavelength = 375 nm), Abs is the absorbance of QDs and standard at 375 nm, and η is the refractive index of the solvent.

1.14 Preparation of Nanoprobes: AuNP and QD functionalization with antibodies

The CdTe-MPA QDs and gold nanoparticles were functionalized with antibodies: 1mL of NP suspension (3.3 nmol) was mixed with 0.4 mg of EDC and 0.8 mg of Sulfo-NHS in PBS buffer pH 7.4, and the mixture was incubated at 37°C for 30 min. The activated NPs solution

was applied to a PD-10 column (GE Healthcare Life science, Ireland) using 10mM PBS pH 7.4 as the exchange buffer. Then 0.6 nmol of IgG antibody was added to 1 nmol of NPs and the mixture was stirred at 37°C for 1 h. Subsequently, the activated carboxylic groups were blocked with 5 mg of 4-Aminophenyl β -D-galactopyranoside, and the mixture was incubated overnight in a final volume of 1.5 mL. NPs conjugated with antibodies (final concentration = 650 nM) were stored at 4 °C. Non-denaturing polyacrylamide gel electrophoresis (PAGE) was used to determine the conjugation of the NPs with the antibody. The photoluminescence spectra of the QDs were recorded in order to analyze any variation in the photoluminescence properties of the functionalized QDs.

1.15 Epitope Mapping

For the immuno-gold (IG) epitope mapping, 90 µg of mono- or bi-functional SiNP-protein conjugates were mixed with increasing amounts of IG to a final concentration of 1 $mg*mL^{-1}$, and incubated at 37 °C for 1 h, under constant agitation. IG functionalized with anti-R Phycoerythrin antibody were used as control for unspecific binding (Figure S11). Samples were then analyzed by DCS. In order to prepare samples for the TEM imaging, 5 washing steps in PBS by centrifugation at 16000 rcf were done to remove the unbound IG before fixation. After 5 additional washing steps in water by centrifugation at 16000 rcf, 5 µL of each sample was dried on formvar-coated copper grids (Agar Scientific, UK, 400 mesh).

For the immuno-QD (IQD) epitope mapping experiments, 120 µg of mono- and bifunctional SiNP-Tf-EGF (synthesized using strategy A, $PEG_{(40)}$ protein linker, $PEG_{(80)}$ backfilling, final concentration 1 $mg*mL^{-1}$) conjugates were mixed with several amounts of IQDs. After 1 h incubation at 37 °C under constant agitation, the samples were centrifuged 3 times at 18000 rcf for 20 minutes and resuspended in fresh PBS to remove the unbound immunolabels. QDs

functionalized with Bovine Serum Albumin were used as control for unspecific binding (Figure S11). Nonfluorescent SiNPs have been used as core particles to avoid interference with the fluorometric analysis of IQDs. The samples were then analyzed by fluorescence spectroscopy and flow cytometry.

1.16 Receptor-specific cellular uptake of SiNPs

Cell culture

Human Embryonic Kidney 293 (HEK-293) cells were cultured in Dulbecco's Modified Eagle's Medium (DMEM) Glutamax (GIBCO, Thermo Scientific, Ireland), supplemented with 10 % Fetal Bovine Serum (FBS) (GIBCO, Thermo Scientific, Ireland) in a humidified chamber at 37°C under 5 % CO_2. Cells were grown and passaged three times a week, as they approached 70 -80 % surface coverage.

Vectors for transfection

The plasmid vectors used were FHC01759 Transferrin receptor (TFR), FHC09683 Epidermal growth factor receptor (EGFR) and FHC10149 oxidized low density lipoprotein (lectin-like) receptor (LOX), purchased from KAZUSA DNA Research Institute (KAZUKA, Japan). All vectors contain a resistance cassette (Ampr) which allows selection of transfected cells by administering the antibiotic Ampicillin.

Bacterial transformation

DH5-alpha Competent E. coli (Subcloning Efficiency) was purchased from New England Bio-Labs (New England Bio-Labs, UK, product no. C2988). Bacteria were transformed with the mentioned plasmid vectors. Bacteria were thawed on ice and incubated with the plasmids of interest for 30 mins. The bacteria was subjected to a heat shock treatment at 42°C for 45 seconds, then rested on ice for 2 mins and then grown in 800 µL of Super Optimal broth with Catabolite repression (SOC Outgrowth Medium, New England BioLabs, UK) for 1 h at 37°C

to allow recovery. 100 µL was spread on a 2XYT-Broth (MP Biomedicals, USA, product no. 3012-032) 2 % agar plates supplemented with Ampicillin (100 µg*mL^{-1}); facilitating selective growth of colonies that incorporate the plasmid DNA, and grown, inverted for 12-18 h at 37°C.

DNA amplification and purification

A colony was transported from the agar plate to a sterile bottle containing 200 mL 2XYT-Broth supplemented with Ampicillin. This was shaken for 12-18 h at 37°C. DNA was purified from the resulting liquid culture. PureYieldTM Plasmid MidiPrep System (Promega, USA, product no. A2495) was used according to manufacturer's instructions to purify DNA. DNA concentration was determined by NanoDrop 2000 UV-Vis spectrophotometer (Thermo Scientific, Ireland.

Transfection of HEK-293 cells

HEK-293 cells were plated 24 h before transfection at a density of 52,000 cells/well into a 24-wells plate (Cellstar® Greiner Bio-One, Germany) in 1 ml of completed medium DMEM Glutamax (GIBCO, Thermo Scientific, Ireland) supplemented with 10 % FBS. After 24 h cells were transfected using FuGENE® 6 (Promega,USA)-to-DNA ratio of 3.5:1 for TFR, EGFR, LOX and empty vector. Plasmid DNA (0.02 µg*µL^{-1}) was added to a sterile tube containing Opti-MEM medium (GIBCO, Thermo Scientific, Ireland). FuGENE® 6 reagent was added to the solution and mixed carefully by pipetting 15 times. The solution was incubated at room temperature for 10 min. 25 µl was then gently added drop wise onto each well and incubated for 48 h at 37 °C and 5 % CO_2.

Cellular uptake

To expose the cells to the nanoparticles solution, after 48 h of the transfection, cells were washed for 30 min in serum-free DMEM. The medium was then replaced by the nanoparticles dispersions, freshly prepared: 0.1 mg*mL^{-1} of SiO_2 nanoparticles were dispersed in serum-free DMEM and in DMEM supplemented with 10 % FBS prior addition to cells. Cells were

exposed to nanoparticles solutions for 4 h at 37 °C and 5 % CO_2. After 4 h incubation, cells were washed twice with DMEM supplemented with 10 % FBS and twice with PBS. Then the cells were harvested with trypsin. Cell pellets were fixed at room temperature with 4% formalin (Sigma-Aldrich, Ireland) for 20 min, and re-suspended in PBS. Cells were analysed using an AccuriTM C6 Flow cytometer (BD Biosciences, UK). At least 15,000 cells were analyzed in each sample.

1.17 Flow cytometry

Flow Cytometry was carried out using a BD AccuriTM C6 cytometer (BD Biosciences, UK).

1.18 Fluorescence spectroscopy

Fluorescence Spectroscopy experiments were performed with a Jobin Yvon Fluorolog-3 (Horiba, UK) fluorimeter using a 45 µL quartz Ultra-Micro cuvette of 3 mm path length (Hellma Analytics, Germany).

1.19 Transmission electron microscopy

Transmission electron microscopy (TEM) micrographs of SiNPs were obtained in a FEI™ Tecnai™ G2 20 Twin microscope (FEI, Inc., The Netherlands) at an accelerating voltage of 200 kV. 5 µL of diluted SiNPs suspensions were dried and analyzed on Formvar/Carbon copper grids (300 mesh, Ted Pella Inc., UK).

1.20 Dynamic light scattering

Dynamic Light Scattering (DLS) measurements were carried out at a typical nanoparticle concentration of 50 µg mL-1 in a 1 mL polystyrene or glass cuvette. Measurements are an

average of three individual runs with 10-15 accumulations per run. Samples were analyzed on a Malvern Nanosizer ZS Series (Malvern, Ireland) at a temperature of 25°C.

1.21 Differential centrifugal sedimentation

Differential Centrifugal Sedimentation (DCS) was carried out using a CPS disc centrifuge DC24000 (CPS Instruments Inc., UK) in which an 8-24 w/w % sucrose-based gradient in PBS water was applied. Measurements were conducted at a speed of 18000 rpm. Calibration was performed using polyvinylchloride (PVC) standard (0.476 μm, Analytik Ltd., UK). Calibration was carried out before each measurement using 0.1 mL of the standard; similarly, 0.1 mL of each sample was injected for the analysis using a calibrated syringe (Hamilton GASTIGHT®, Hamilton, UK) with an accuracy of ±1 % within the injected volume.

1.22 UV-Vis spectroscopy

UV-Vis spectra were recorded on a Varian's Cary®6000i spectrophotometer (Agilent Technologies, Ireland) using a quartz cuvette with a path length of 1 cm at a typical SiNP concentration of 500 $\mu g^{*}mL^{-1}$.

2. Supporting data

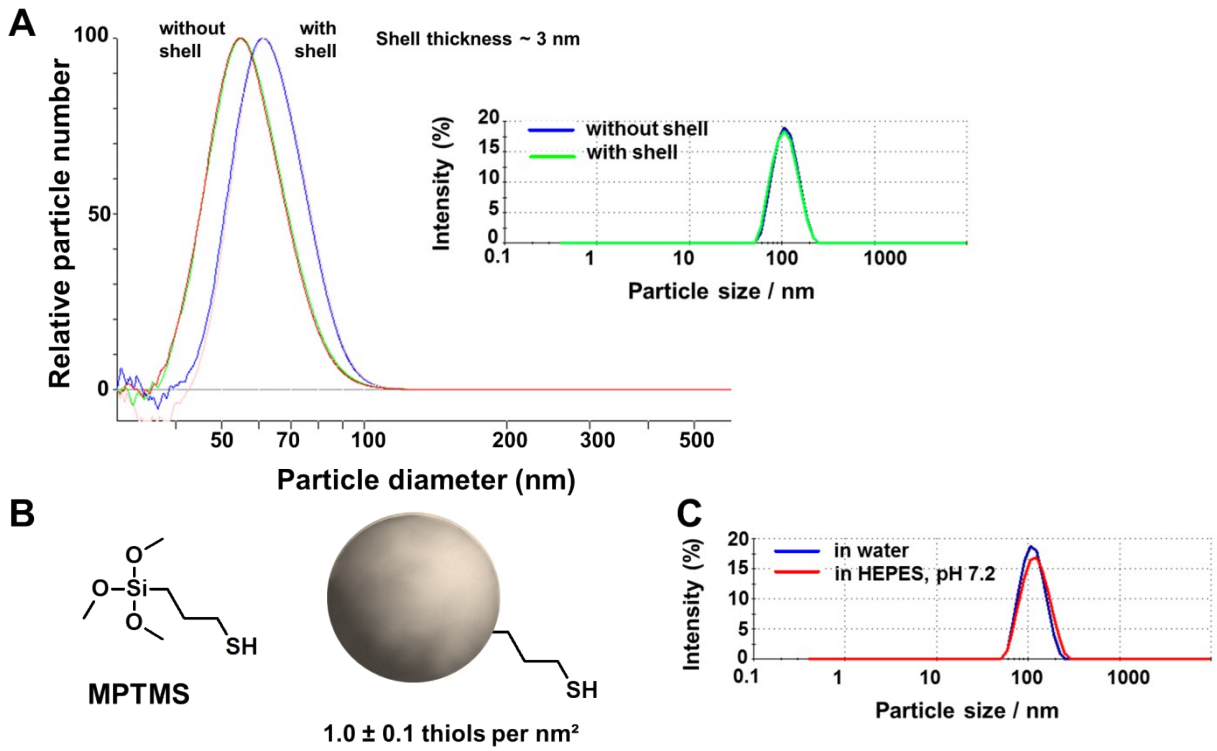

Figure S1. Characterization of SiNP core particles. a) The fluorescent core of the particle was protected by a silica shell. DCS and DLS (inset) measurements of particles before and after growth of a silica shell. From the DCS measurements a shell thickness of about 3.5 nm can be observed. Further characterizations of the core and its fluorescence properties can be found in ref. [1]. b) Structure of MPTMS and schematic of thiol-functionalized SiNPs, the number of reactive thiols per nm² after functionalization was usually 1.0 ± 0.1 per nm² and determined via Ellman's assay. c) DLS of thiol-functionalized SiNPs in water and in HEPES buffer in which protein conjugation is conducted. The particles show single peaks that are found at about the size of the SiNPs core shell particles and low polydispersity indices (PDI) of 0.09 and 0.07 in water and HEPES, respectively suggesting stable dispersions.

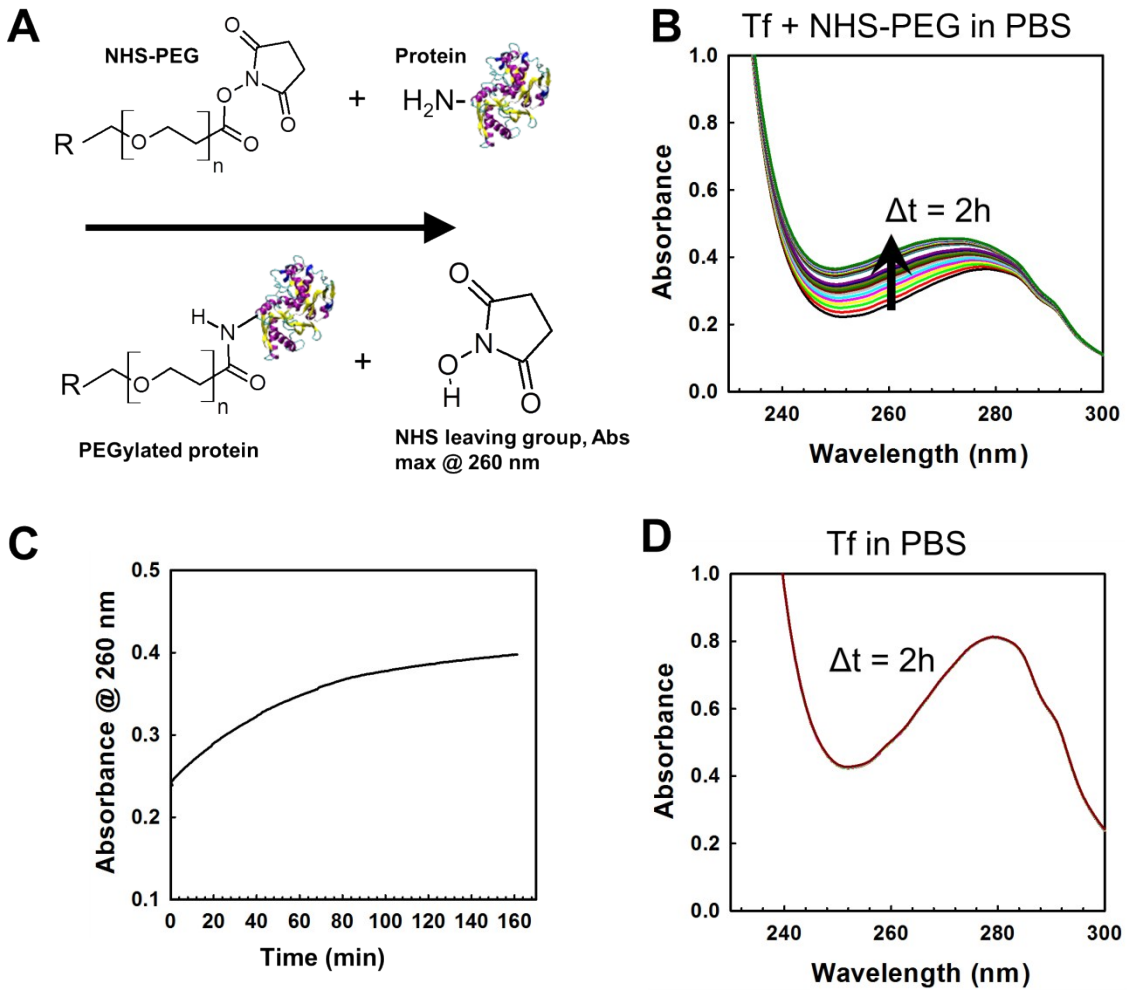

Figure S2. PEGylation of proteins. a) Schematic of the PEGylation of proteins for conjugation onto SiNPs (R = maleidmide or DBCO which links the protein onto the particles). b) UV-Vis spectra of the PEGylation of Tf with NHS-$PEG_{(8)}$-maleimide. An increase of the absorbance can be observed overtime due to the release of the NHS leaving group upon reaction of NHS-PEG-R with the amine on the protein. c) Absorbance at 260 nm over time shows saturation at about 120 min suggesting completeness of reaction, thus all PEGylagtion reactions have been conducted for 120 min. d) Tf in PBS measured over 120 min does not show any variation in the signals (curves overlay). The UV-Vis spectra for NHS-PEG-maleimide in PBS (data not shown) shows increase in the signal due to the hydrolysis of the NHS functionality and release of the NHS leaving group, however, if amines are present, the reaction with amines is favored and contribution of hydrolysis negligible [11].

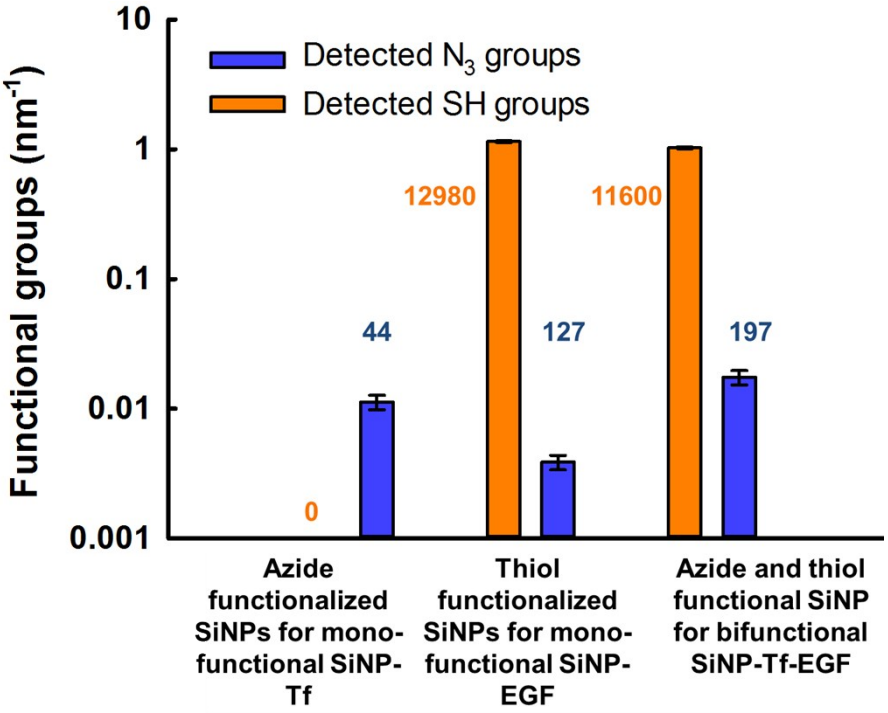

Figure S3. Number of reactive thiol and azide groups on functionalized SiNPs for linking strategy B in which Tf is bound *via* the DBCO-azide pair and EGF *via* maleimide-thiol pair to reduce competition of the proteins for the same linking group. Thiol groups were determined with Ellman's assay and azide groups by fluorescence after reaction with DBCO-Cy5.5. The orange and blue numbers represent the number of thiol and azide functional groups, respectively per SiNP. No thiol groups were expectedly detected on the azide functionalized core SiNPs (for monofunctional SiNP-Tf). Although thiol-functionalized SiNPs (for monofunctional SiNP-EGF) were not functionalized azide groups, the DBCO-Cy5.5 assay gives a signal for those particles (blue bar) which is likely nonspecific interaction of the DBCO-Cy5.5 with the thiol-functionalized SiNPs and can be considered as background signal of the assay. SiNPs functionalized with both, azide and thiol groups (for bifunctional SiNP-Tf-EGF) show higher azide groups than that "background". Subtracting the signal for azide groups of the thiol-functionalized SiNPs number per SiNPs (127 azides per SiNP) from that of the thiol- and azide-functionalized SiNPs (197 azides per SiNP) results in 70 azides per SiNP which is of similar magnitude to 44 azides per SiNP measured on azide-functionalized

SiNPs without thiols. The number of reactive thiol groups on the particles is higher which could have several reasons. First, the silanization reaction for MPTMS is more efficient than for N3PTES, second, not all of the azide groups react with the DBCO-Cy5.5 molecule. Interestingly, the number of reactive azide groups, 44 per SiNP (for monofunctional SiNP-Tf) and 70 per SiNP (for bifunctional SiNP-Tf-EGF), corresponds almost exactly to the number of covalently conjugated Tf on those particles which is 49 Tf per SiNP and 57 Tf per SiNP (calculated from Figure S3b). The thiol groups per particle are about 1000 (monofunctional SiNP-EGF) to 40 (bifunctional SiNP-Tf-EGF) times higher than the bound EGF amounts suggesting that a majority remains after protein conjugation that were backfilled with maleimide-PEG_4-OH.

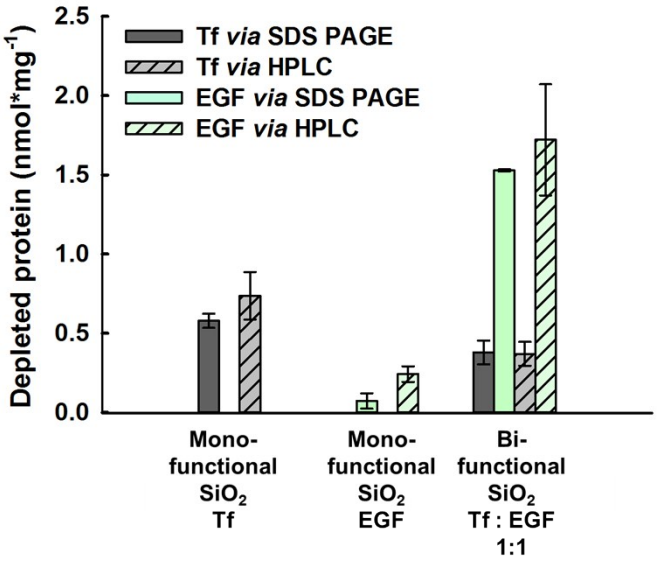

Figure S4. Comparison of determination of Tf and EGF on mono- and bifunctional SiNP-Tf-EGF conjugates via SDS-PAGE (quantification of depleted protein after reaction) and HPLC (quantification and numerical analysis of amino acid profiles obtained from SiNP-conjugated EGF and Tf by acid digestion). Both techniques show widely comparable results.

Table S2. Size and polydispersity index (PDI) of core SiNPs in HEPES (medium of protein conjugation) and protein conjugated SiNPs in PBS, illustrated in Fig.1c, and Fig. 1e of the main manuscript. The error represents the standard deviation of three to five measurements per sample.

DLS characterization mono and bifunctional NPs in PBS				
Linking strategy A, no backfilling				
	Z-average (nm)	PDI	Intensity mean (nm)	Number mean (nm)
SiO_2 core (in HEPES)	101 ± 1	0.08	110 ± 2	74 ± 3
Monofunctional SiO_2 - Tf	124 ± 2	0.10	139 ± 4	87 ± 5
Monofunctional SiO_2 - HSA	201 ± 2	0.26	263 ± 24	78 ± 36
Bifunctional SiO_2 - Tf : HSA 1:1	137 ± 1	0.12	157 ± 2	92 ± 4
Bifunctional SiO_2 - Tf : HSA 3:1	130 ± 1	0.13	151 ± 3	82 ± 5
Linking strategy B, $PEG_{(4)}$ backfilling				
	Z-average (nm)	PDI	Intensity mean (nm)	Number mean (nm)
SiO_2 core (in HEPES)	113 ± 2	0.06	123 ± 2	85 ± 3
Monofunctional SiO_2 - Tf	1273 ± 347	0.27	1721 ± 527	1157 ±319
Monofunctional SiO_2 - EGF	1116 ± 191	0.26	1438 ± 264	1065 ± 219
Bifunctional SiO_2 - Tf : EGF 1:1	195 ± 3	0.20	236 ± 9	116 ± 15
Linking strategy A, $PEG_{(80)}$ backfilling				
	Z-average (nm)	PDI	Intensity mean (nm)	Number mean (nm)
SiO_2 core (in HEPES)	114 ± 2	0.08	124 ± 2	79 ± 2
Monofunctional SiO_2 - Tf	109 ± 1	0.02	113 ± 1	89 ± 1
Monofunctional SiO_2 - EGF	110 ± 1	0.02	115 ± 1	90 ± 2
Bifunctional SiO_2 - Tf : EGF 1:1	112 ± 1	0.02	119 ± 1	89 ± 3

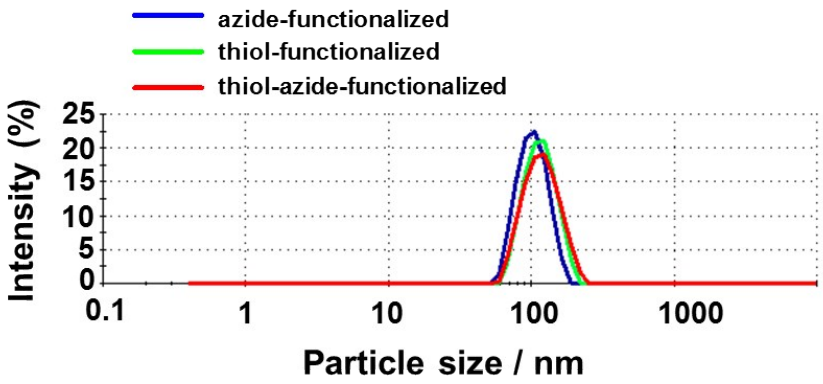

Figure S5. Stability of thiol and azide functionalized SiNPs in HEPES buffer at pH 7.2 before addition of the proteins. The PDIs are 0.04, 0.07, and 0.06 for azide-functionalized, thiol-functionalized, and thiol-azide-functionalized SiNPs, respectively, confirming that the NPs are stable at the conditions of protein conjugation.

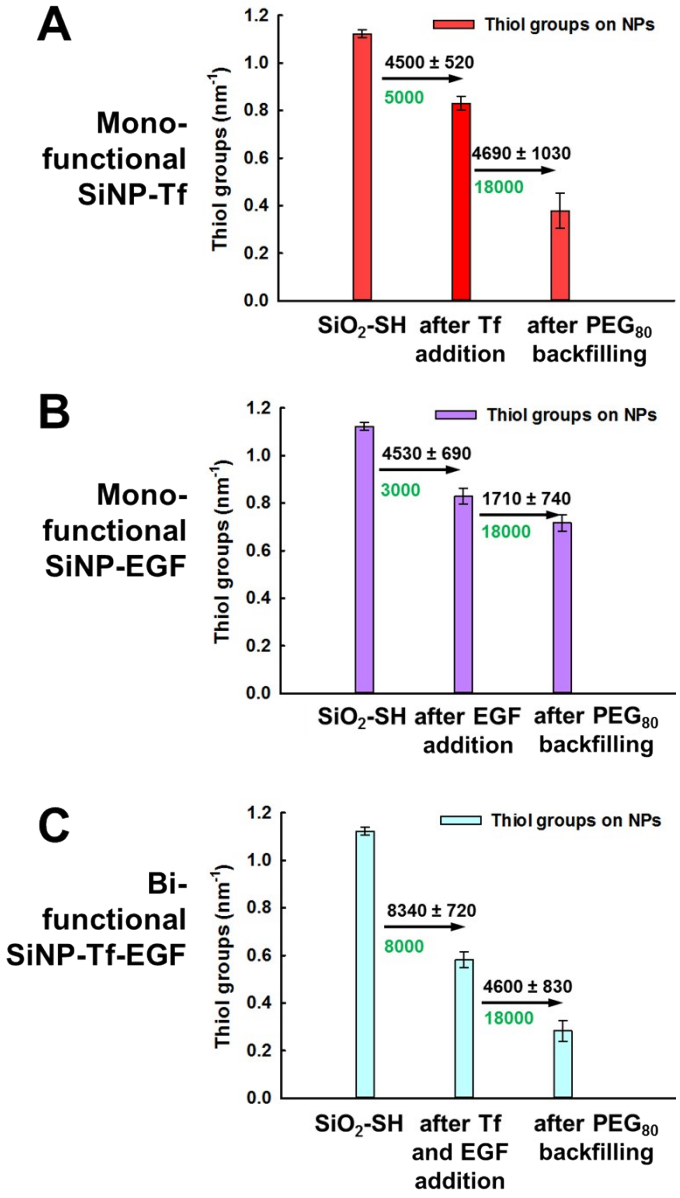

Figure S6. Number of thiol groups after conjugation of protein and PEG-backfilling (linker strategy A, protein conjugated *via* maleimide-$PEG_{(40)}$-NHS, backfilling *via* maleimide-PEG_{80}-OH). The black numbers in the charts are the thiol groups per SiNPs that were consumed during reaction obtained by subtracting the measurements. The green numbers is the amount of maleimide-PEG added for the reaction. a) Shows data for synthesis of monofunctional SiNP-Tf, b) for monofunctional SiNP-EGF, anc c) for bifunctional SiNP-Tf-EGF. The number of thiol group reduces after protein conjugation and the number of consumed thiol groups per SiNP-protein conjugates corresponds to the number of added PEG during protein conjugation for a), b) and c) (number of added PEG is 10 fold higher for Tf and 3 fold higher

for EGF, than the Tf and EGF conjugation respectively). For backfilling an excess of maleimide-$PEG_{(80)}$ is added and reduction of thiol groups is observed confirming consumption of thiols due PEG conjugation during backfilling. Not all of the backfilling PEG is consumed and some thiol groups remain after backfilling potentially because they are not accessible for the PEG molecules due to the already grafted proteins. Nevertheless, the consumption of thiols confirm the successful conjugation of proteins and backfilling PEG for all particles and insights in surface reactivity of the SiNPs.

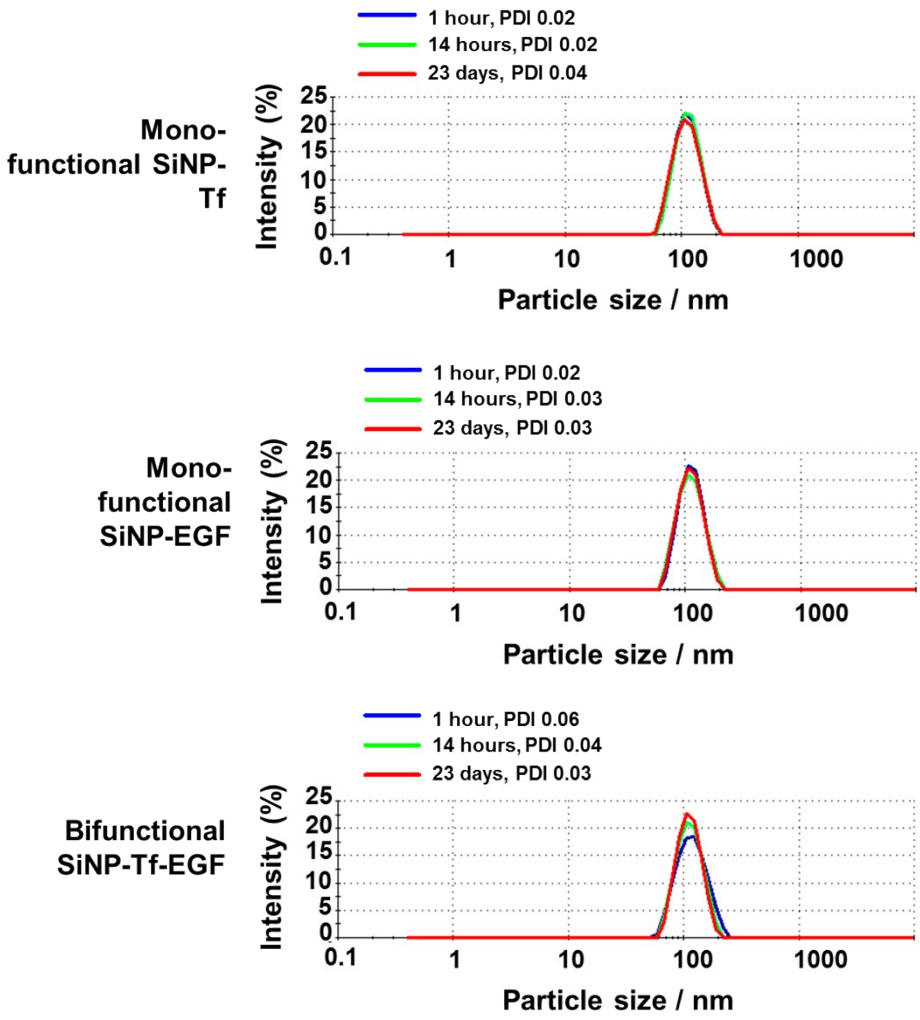

Figure S7. DLS of monofunctional SiNP-Tf, monofnctional SiNP-EGF, and bifunctional SiNP-Tf-EGF (linker strategy A, proteins conjugated *via* maleimide-$PEG_{(40)}$-NHS, maleimide-$PEG_{(80)}$ backfilling) after storage of up to 23 days in PBS at 4°C. The monomodal

size distributions and low PDIs suggest highly stable SiNP-protein conjugate dispersions after $PEG_{(80)}$ backfilling.

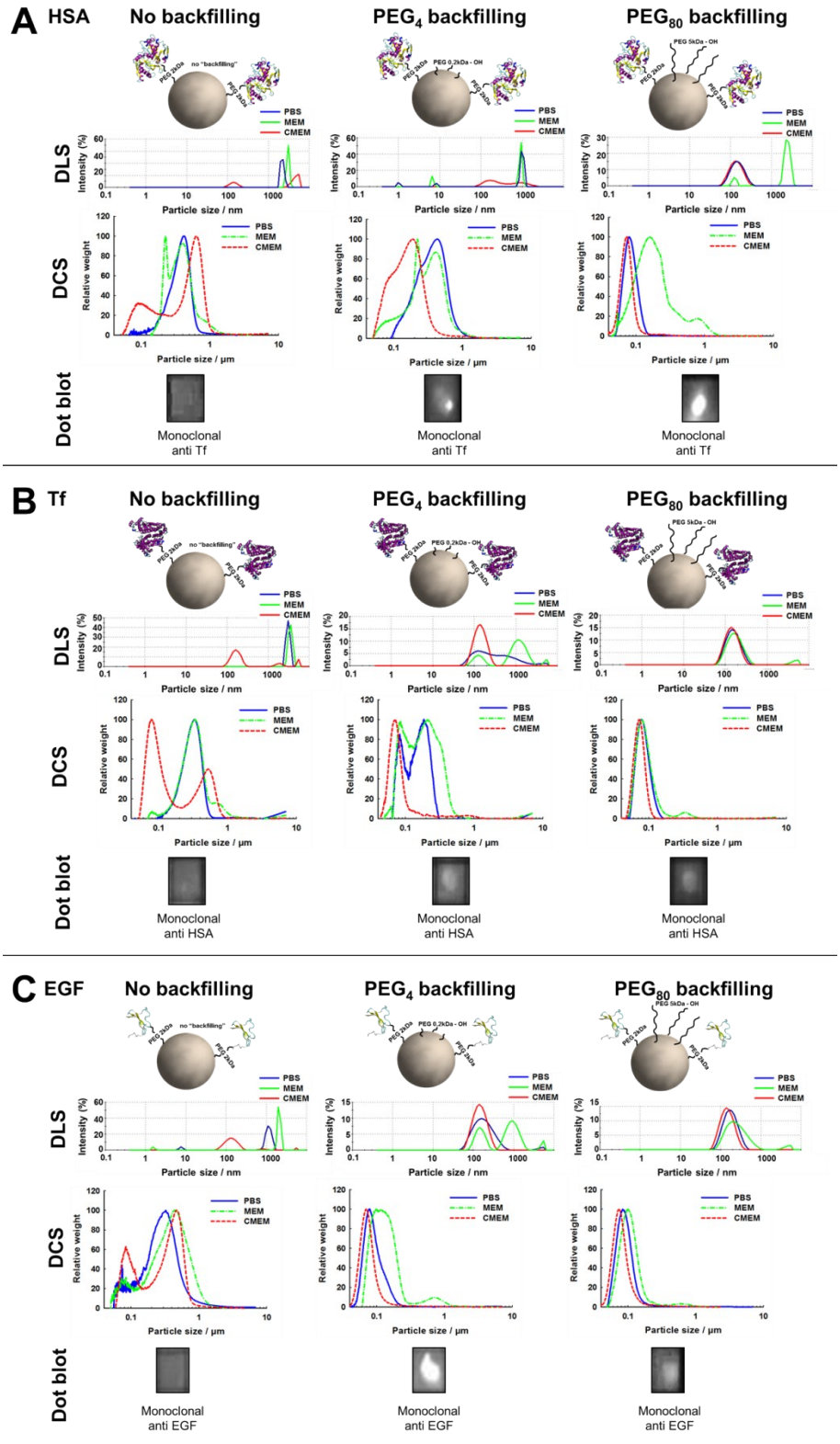

Figure S8. Improving SiNP-protein conjugate stability against aggregation in different biological media (PBS, minimum essential medium (MEM) and MEM supplemented with 10 % fetal bovine serum (cMEM) by different type of backfilling. The figure compares DLS and DCS measurements measured 4h after exposure to the media of SiNP-conjugates with a) HSA, b) Tf, and c) EGF (all linker strategy A using a $PEG_{(40)}$-maleimie) for either no backfilling, backfilling with a maleimide-$PEG_{(4)}$-OH or maleimide-$PEG_{(80)}$. The measurements show increased stability by monomodal and narrow size distributions of all SiNP-protein conjugates after $PEG_{(80)}$ backfilling in PBS and cMEM and for SiNP-EGF and SiNP-Tf in MEM showing strongly increased stability while PEG_4 and no backfilling leads to poor stability. The dot blots confirm that the particles after $PEG_{(80)}$ backfilling show specific recognition by monoclonal antibodies. No recognition is shown for not-backfilled SiNP-protein conjugates possibly due to a strong decrease of surface exposed recognition sites after aggregation.

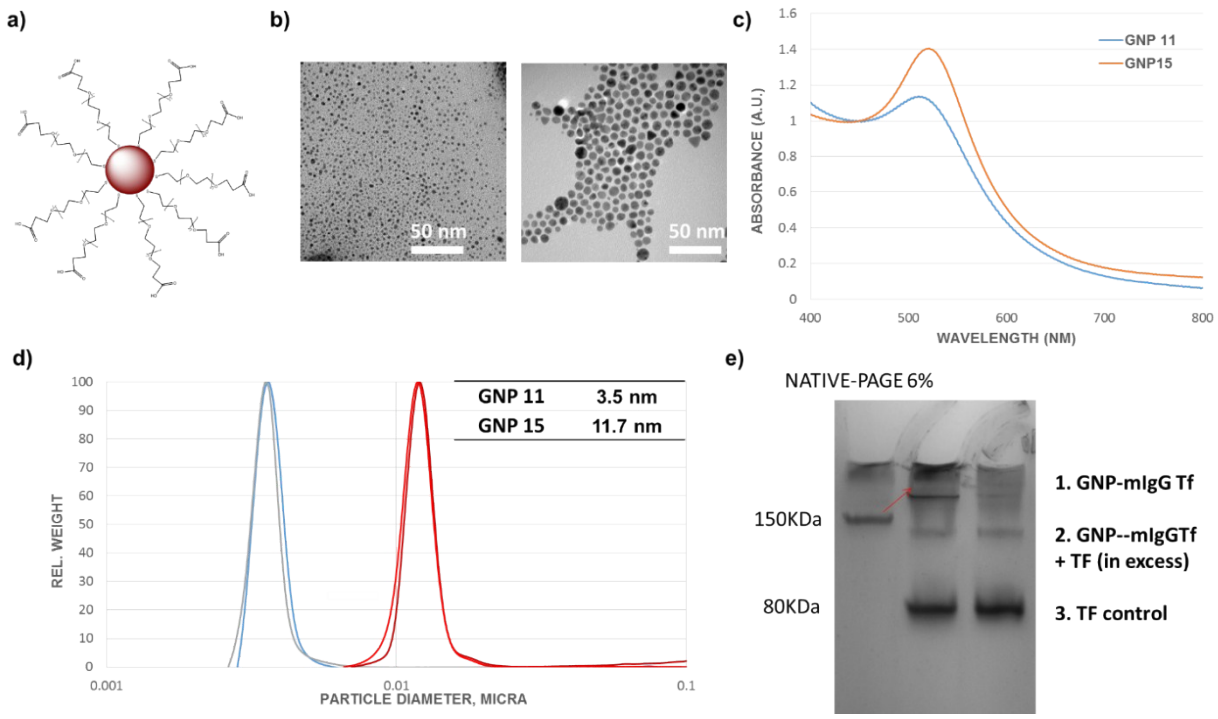

Figure S9. Characterization of AuNPs-antibody conjugates. a) Schematic representation of gold nanoparticle functionalized with O-(2-Carboxyethyl)-O'-(2-mercaptoethyl)

heptaethylene glycol (SH-PEG-COOH, MW= 458.56 g/mol), used for the immunolabelling process. To distinguish two different proteins on bifunctional SiNPs in TEM, a ~3nm AuNPs and ~11nm AuNPs have been selected as their size distributions do not overlap. b) TEM micrographs of ~3nm AuNPs (left) and ~11nm AuNPs (right). c) UV-Vis spectra of of ~3nm AuNPs (blue) and ~11nm AuNPs (red). d) Size distributions of differently sized AuNPs measured in DCS (3nm AuNPs (blue) and ~11nm AuNPs (red)). e) Native PAGE gel electrophoresis (6%) of monoclonal anti-Tf antibody bound to 3.5 nm AuNPs before and after incubation with a Transferrin solution. Further characterization will be found in ref [12].

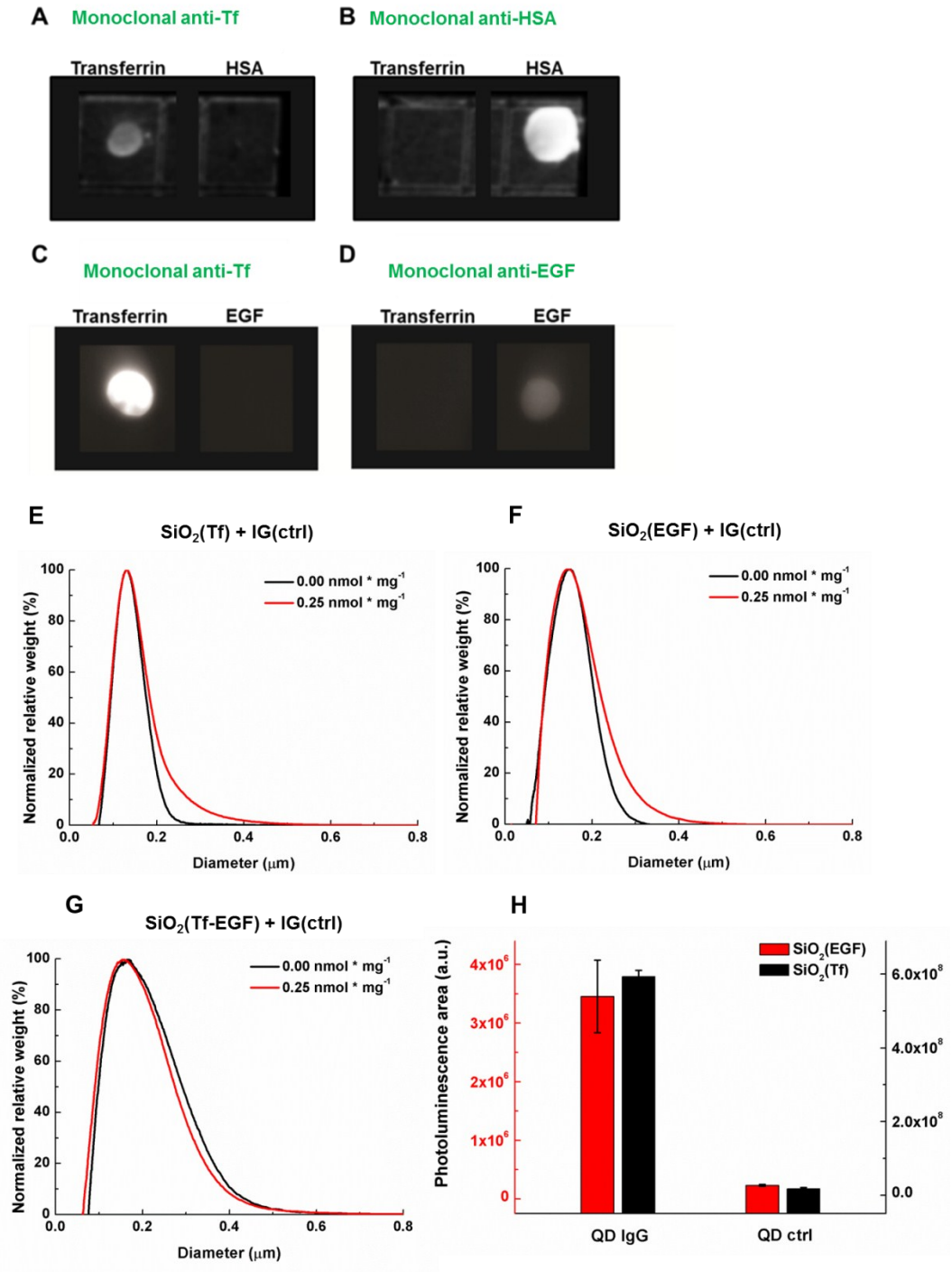

Figure S10. Dot blots testing cross reactivity and unspecific binding for the different antibodies used. a) Monoclonal anti-transferrin showing positive transferrin binding and no HSA binding. b) Monoclonal anti-HSA showing no binding for transferrin and positive HSA binding. c) Monoclonal anti-transferrin showing positive transferrin binding and no EGF binding. d) Monoclonal anti-EGF showing no Transferrin binding and a strong EGF signal.

The data suggests that cross-reactivity and unspecific binding between the antibody-antigen couples is negligible. e) DCS analysis of SiNP-Tf (e), SiNP-EGF (f) and SiNP-Tf-EGF (g) incubated with 0.25 nmol of IGctrl (QDs without antibody) per silica NP. No shift in the position of the SiNPs peak is observed, indicating that the fraction of unspecific binding is negligible. h) Comparison between the fluorescence spectroscopy analysis of SiNP-EGF (red) and SiNP-Tf (black) mapped with saturating concentration of IQDEGF and IQDTf respectively (first two columns), and the same NPs incubated with IQDctrl.

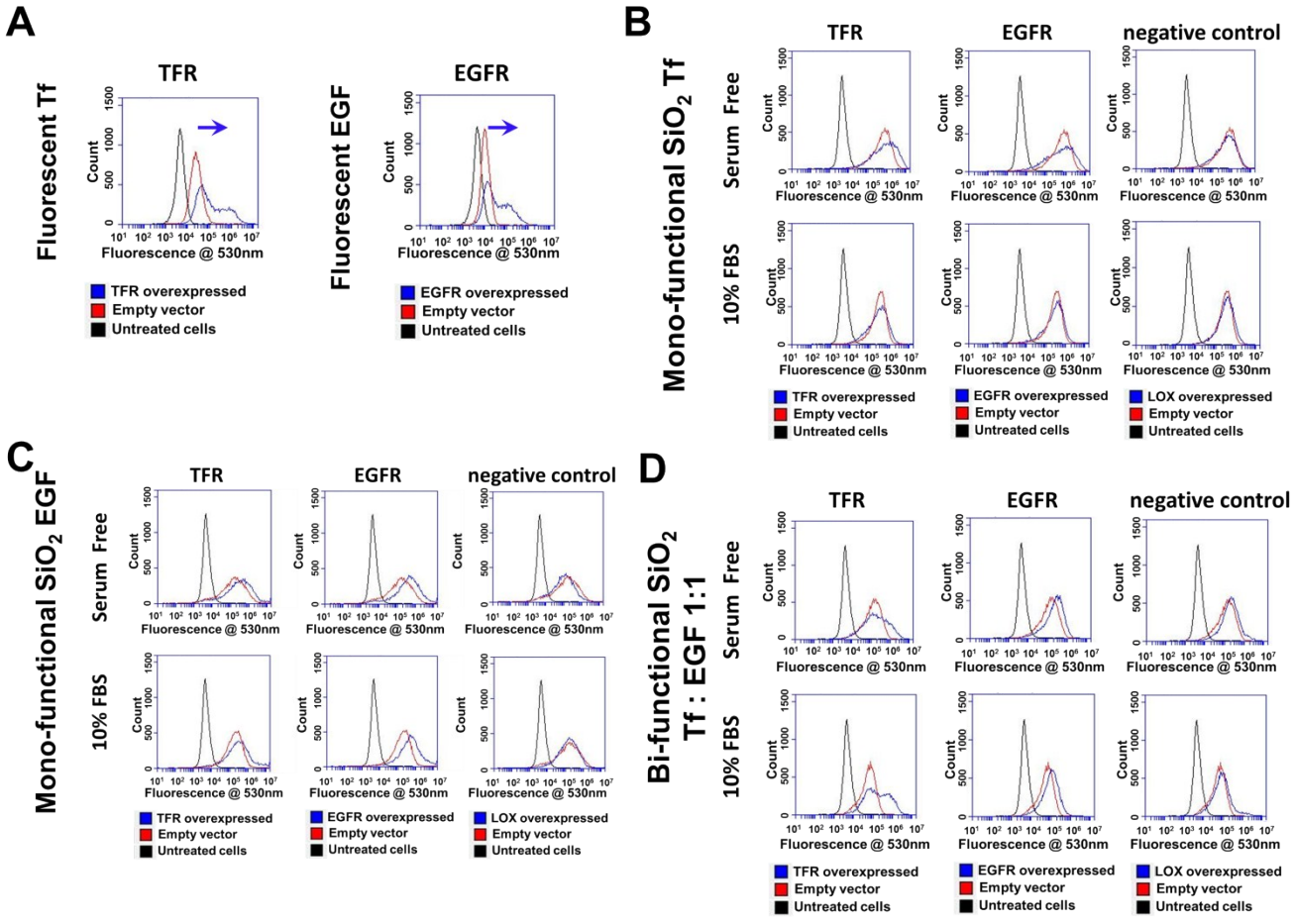

Figure S11. Cellular uptake study of functional SiNP-Tf-EGF conjugates in transfected HEK-293 cells. SiNP-protein conjugates were dispersed in serum free media and in media supplemented with 10 % FBS prior addition to cells. Cells were incubated with nanoparticles

solution at 0.1 mg*mL^{-1} for 4 h at 37°C. a) Uptake of fluorescent labeled Tf-AlexaFluor488 in TFR-transfected HEK-293 cells and fluorescent labeled EGF-AlexaFluor488 in EGFR-transfected HEK-293 cells (blue lines) as well as in cells treated with an empty transfection vector to obtain reference cells that do not overexpress TFR or EGFR (red lines). The histograms of uptake in transfected cells are shifted towards increased fluorescence at 530 nm (indicated by blue arrow) for both, Tf and EGF, when compared with empty vector transfected cells. This suggests increased uptake of Tf or EGF when cells overexpress TFR and EGFR and the results confirm an successful transfection of the cells. b) Uptake of monofunctional SiNP-Tf in TFR-transfected and EGFR-transfected cells in serum free and in 10 % FBS. The particles were also incubated with LOX-transfected cells as a negative control. The data (shift of histogram for transfected cells compared to cells treated with empty vector) suggest increased uptake in cells overexpressing Tf and EGF but the uptake is slightly higher in Tf overexpressed cells proposing a Tf specific uptake path. This is lost in media containing even low FBS concentrations as also observed previously.[13] c) Uptake of monofunctional SiNP-EGF in TFR-transfected and EGFR-transfected cells in serum free and in 10 % FBS media (LOX-transfected cells as a negative control). The data (shift of histogram for transfected cells compared to cells treated with empty vector) suggests increased uptake in cells overexpressing EGF and Tf receptors which is higher for cells overexpressing the EGF receptor and the effect remains in low FBS concentrations (10%) and serum-free media suggesting EGF-specific uptake of the SiNP-EGF conjugates. d) Uptake of bifunctional SiNP-Tf-EGF (1:1) in TFR-transfected and EGFR-transfected cells in serum free and in 10 % FBS. Nanoparticles were exposed to LOX-transfected cells as a negative control. The data suggests increased uptake in cells overexpressing Tf and EGF receptors. The effect remains in media with low serum concentrations and is in case of Tf compared to a) strongly pronounced. This suggests that bifunctional SiNP-Tf-EGF conjugates are up taken *via* Tf-specific and EGF-specific paths showing that both surface molecules are active. For all particles, the negative

control (LOX-transfection) does not increase the uptake of all SiNPs suggesting that an overexpression of the lectin-like oxidized low-density lipoprotein does expectedly not increase SiNP-protein conjugate uptake. Data represent the median of the cell fluorescence intensity. At least 15,000 cells were analyzed in each repeat using BD AccuriTM C6 Flow Cytometer. Blue (cells transfected with: TFR, EGFR, LOX), Red (cells transfected with an empty vector), black (untransfected/untreated cells). All particles used for this experiments were synthesized using linking strategy B, $PEG_{(40)}$ protein linker, and $PEG_{(4)}$-OH backfilling.

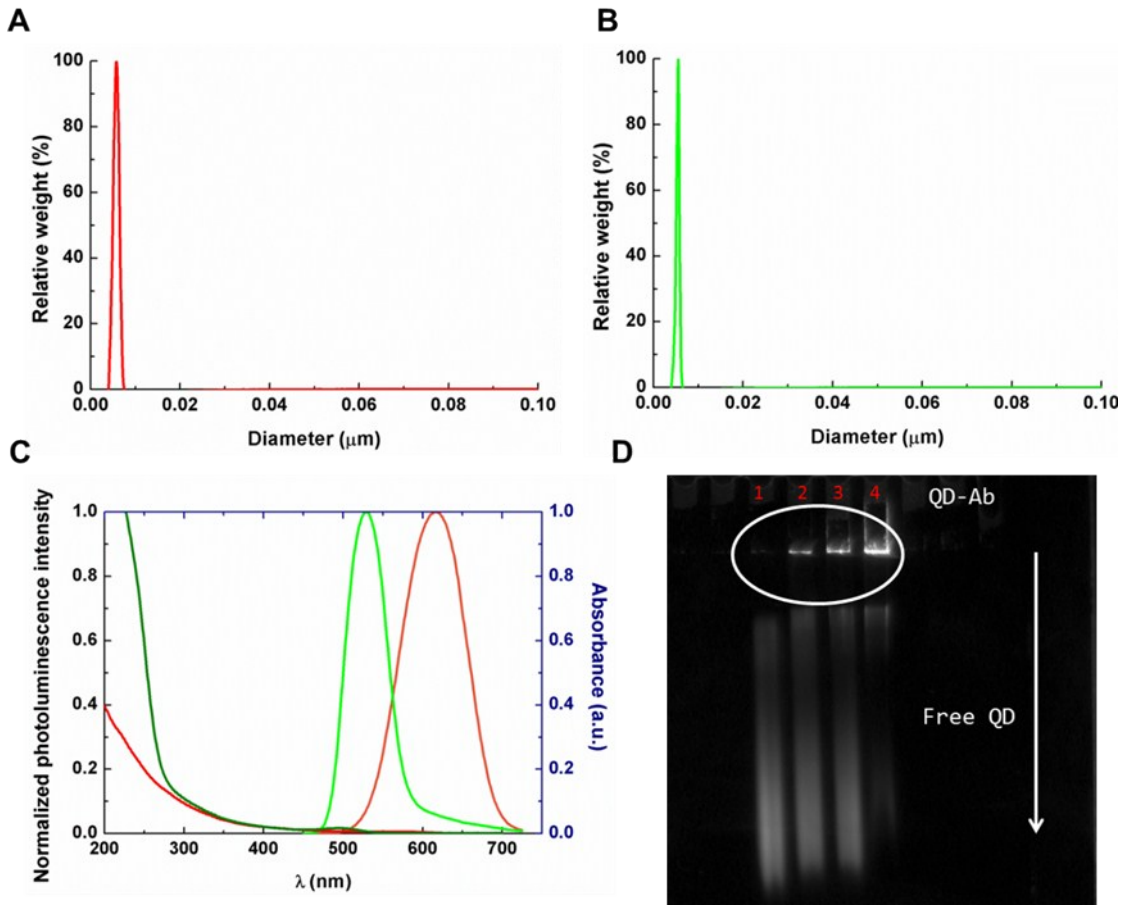

Figure S12. Quantum Dots characterization. a) DCS characterization of orange emitting QDs (5.8 nm) b) DCS characterization of green emitting QDs (5.5 nm). c) UV-Vis and fluorescence spectra of orange emitting QDs (dark and light red line, respectively) and green

emitting QDs (dark and light green line, respectively). The maximum emission wavelength was found at 615 nm and 530 nm for the orange and green QDs, respectively. All the spectra were recorded using 375 nm as excitation wavelength. d) Fluorescence scan of a native PAGE of orange emitting QDs conjugated with different amount of monoclonal antibody against Transferrin (0, 0.2, 0.4, 0.6 antibody to QD molar ratio for line 1, 2, 3 and 4, respectively. The unconjugated QDs can be distinguished from the ones conjugated to antibodies (QD-Ab) from the speed at which they travel in the gel. For the bioconjugation, we used the 0.6 antibody/QD molar ratio, since they shows lower amounts of free QDs and a ratio of 0.6 minimizes the chance of having more than an antibody conjugated per QD.

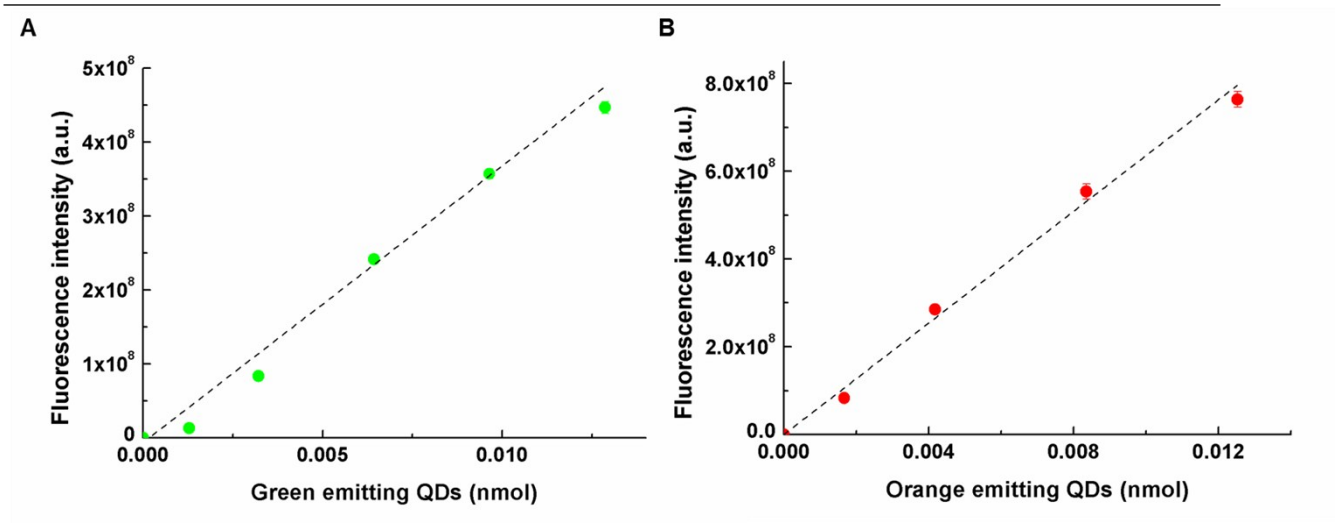

Figure S13. Estimation of the number of exposed epitopes by fluorescence spectroscopy. In order to estimate the amount of EGF and Tf epitopes on bifunctional NPs, the photoluminescence peak of the IQD treated samples was compared with a QD calibration curve, under the assumption that the total fluorescence of the sample with a certain number of IQDs is equivalent to the amount of fluorescence intensity of a solution of known QDs concentration. A. calibration curve for green emitting IQDs. Linear fitting analysis ($y = ax + b$, $a = 3.7^{10}$, $b = -2.0^{7}$ and R-square 0.99). B. calibration curve for orange emitting IQDs. Linear fitting analysis ($y = ax + b$, $a = 6.4^{10}$, $b = 0$ and R-square 0.99). To estimate the number of epitopes, we ignore any filter effects that the presence of proteins or SiNPs may cause.

Nevertheless, the emission peaks of both QDs do not overlay and thus allow a separate quantification. Although our results do not suggest such an effect, it needs to be considered, that the nanoprobes may underestimate the number of epitopes in case of any influences of the QDs on the antibody binding efficacy. Assuming, however, that this error is constant when mapping different samples with the same type of IQDs, the technique proves to be adequate to obtain information on the complex distribution of recognition motifs on multivalent NP-protein conjugates.

---

3. Literature

[1] F. Meder, S. S. Thomas, L. W. Fitzpatrick, A. Alahmari, S. Wang, J. G. Beirne, G. Vaz, G. Redmond, K. A. Dawson, *ACS Nano* **2016**.
[2] Y. Huang, J. E. Pemberton, *Colloids and Surfaces A: Physicochemical and Engineering Aspects* **2010,** *360*, 175-183.
[3] http://www.rcsb.org/pdb/home/home.do RCSB Protein Data Base. http://www.rcsb.org/pdb/home/home.do (accessed December 2013).
[4] M. P. Monopoli, D. Walczyk, A. Campbell, G. Elia, I. Lynch, F. Baldelli Bombelli, K. A. Dawson, *J. Am. Chem. Soc.* **2011,** *133*, 2525-2534.
[5] K. Salchert, T. Pompe, C. Sperling, C. Werner, *J. Chromatogr. A* **2003,** *1005*, 113-122.
[6] J. Greene, J. W. Henderson, J. P. Wikswo. Rapid and Precise Determination of Cellular Amino Acid Flux Rates Using HPLC with Automated Derivatization with Absorbance Detection **2009**.
[7] T. Cedervall, I. Lynch, S. Lindman, T. Berggard, E. Thulin, H. Nilsson, K. A. Dawson, S. Linse, *Proc. Natl. Acad. Sci. USA* **2007,** *104*, 2050-2055.
[8] N. C. Stellwagen, *Electrophoresis* **1998,** *19*, 1542-1547.
[9] J. Gallo, I. García, N. Genicio, S. Penadés, *Particle & Particle Systems Characterization* **2014,** *31*, 126-133.
[10] L. Zou, Z. Gu, N. Zhang, Y. Zhang, Z. Fang, W. Zhu, X. Zhong, *J. Mater. Chem.* **2008,** *18*, 2807-2815.
[11] G. T. Hermanson, *Bioconjugate techniques*. 2. ed. ed.; Elsevier Acad. Press: **2008**.
[12] M. C. Lo Giudice, L. Herda, E. Polo, K.A. Dawson; , *in preparation*
[13] A. Salvati, A. S. Pitek, M. P. Monopoli, K. Prapainop, F. B. Bombelli, D. R. Hristov,
[14] P. M. Kelly, C. Aberg, E. Mahon, K. A. Dawson, *Nat Nano* **2013,** *8*, 137-143.